JOC*Article*

Two-Dimensional Networks of Ethylenedithiotetrathiafulvalene Derivatives with the Hydrogen-Bonded Functionality of Uracil, and Channel Structure of Its Tetracyanoquinodimethane Complex

Yasushi Morita,*[,†,‡] Eigo Miyazaki,[†] Yoshikazu Umemoto,[†] Kozo Fukui,[‡] and Kazuhiro Nakasuji*[,†]

Department of Chemistry, Graduate School of Science, Osaka University, Toyonaka, Osaka, 560-0043, Japan, and PRESTO, Japan Science and Technology Agency (JST), Hon-cho, Kawaguchi, Saitama, 332-0012, Japan

morita@chem.sci.osaka-u.ac.jp

Received April 10, 2006

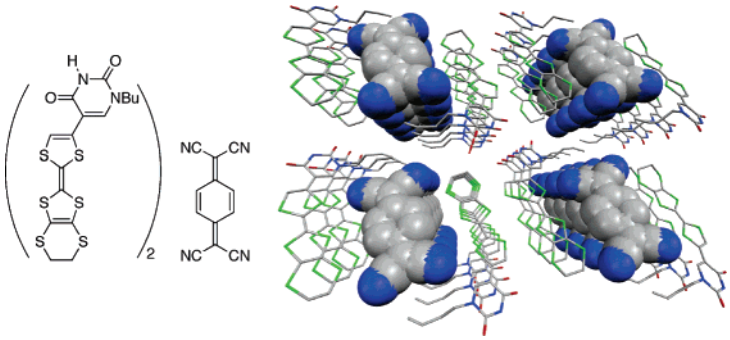

Ethylenedithiotetrathiafulvalene (EDT-TTF) derivatives with N^1-butyluracil or N^1-phenyluracil moiety were designed and synthesized as new hydrogen-bonded electron-donor molecules with the aim of introducing multiple S···S interactions into the hydrogen-bonded structures composed of the TTF−nucleobase systems. In the crystals of the EDT-TTF derivatives, two-dimensional sheet and layer structures were formed through $\pi\cdots\pi$, multiple S···S interactions, and complementary double hydrogen bonds. In the tetracyanoquinodimethane (TCNQ) charge-transfer complex of the EDT-TTF−N^1-butyluracil dyad with a segregated column, a layer structure of the electron-donor molecules was constructed through the noncovalent interactions. The *n*-butyl group of the uracil moiety served to separate the space between the donor layers, resulting in construction of a channel structure. Disordered TCNQ molecules were located in the microporous space of the channel. The TCNQ complex exhibited high electric conductivity ($\sigma_{rt} = 2.1$ S cm^{-1}) in a single crystal.

Introduction

Organic charge-transfer (CT) complexes and salts based on tetrathiafulvalene (TTF) and its derivatives were widely investigated in the field of molecule-based conductive materials science.[1] From the viewpoint of crystal engineering, utilization of the directional and strong hydrogen-bonding (H-bonding) interactions[2] such as NH···N and OH···O is one of the hot topics in the studies of organic conductors.[3] In addition to such a structural effect of the H-bond, we recently demonstrated new roles of the H-bonding interaction: control of electron-donating and -accepting abilities of donor/acceptor molecules and their molecular ratio in the CT complexes of the dibenzo-TTF

* To whom correspondence should be addressed. Phone: +81-6-6850-5393. Fax: +81-6-6850-5395.
† Osaka University.
‡ PREST, JST.

(1) Recent overviews on organic conductors, see: (a) *Organic Superconductors*, 2nd ed.; Ishiguro, T., Yamaji, K., Saito, G., Eds.; Springer-Velrag: Tokyo, 1998. (b) *TTF Chemistry*: *Fundamentals and Applications of Tetrathiafulvalene*; Yamada, J., Sugimoto, T., Eds.; Kodansha and Springer: Tokyo, 2004.

(2) Recent reviews of H-bonding, see: (a) *An Introduction to Hydrogen Bonding*; Jeffrey, G. A., Ed.; Oxford University Press: New York, 1997. (b) *The Weak Hydrogen Bond*; Desiraju, G. R., Steiner, T., Eds.; Oxford University Press: New York, 1999; Chapter 1.

(3) Recent overview on structures and properties of TTF derivatives with H-bonding functionalities, see: Fourmigué, M.; Batail, P. *Chem. Rev.* **2004**, *104*, 5379.

10.1021/jo060748l CCC: $33.50 © 2006 American Chemical Society
Published on Web 06/27/2006

derivative with amino groups[4] and the TTF derivative with imidazole systems.[5] As part of our ongoing studies, we investigated TTF π-systems with nucleobases such as uracil and N^1-butyluracil, TU and T*n*bU,[6] and established the usefulness of the introduction of nucleobases into the TTF π-system to construct highly ordered multidimensional molecular systems based on complementary double H-bonds.[7] Notably, achievement of high electrical conductivities in the tetracyanoquinodimethane (TCNQ) CT complexes of TU and T*n*bU showed an interesting strategy for the construction of H-bonded CT complexes.[6] These stimulative results have encouraged us to study further TTF derivatives with nucleobases.

Chemical modification of the TTF moiety also gives a good opportunity to acquire molecule-based conductive materials with multidimensional networks. It is well-known that the ethylenedithio group of ethylenedithiotetrathiafulvalene (EDT-TTF) can contribute to the formation of a multidimensional network structure by intermolecular interactions through several sulfur atoms.[1] Importantly, in the CT salts of EDT-TTF derivatives with H-bonding functionalities, the intermolecular S···S interactions played a key role in realizing highly conductive H-bonded materials having multidimensional structures with the help of H-bonds.[8,9] Thus, we have newly designed EDT-TTF derivatives with N^1-butyluracil and N^1-phenyluracil moieties, **1a** and **1b**,

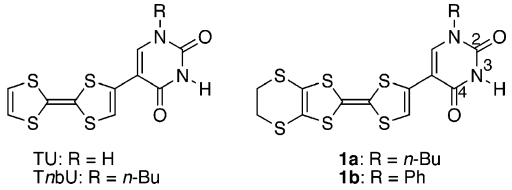

respectively, so as to introduce multiple S···S interactions into H-bonded structures composed of TTF−nucleobase systems. Here we report on the syntheses, structures, and physical properties of **1a**, **1b**, and their TCNQ CT complexes, revealing two-dimensional networks for **1a** and **1b**, and a channel structure for (**1a**)$_2$−TCNQ with high electric conductivity (σ_{rt} = 2.1 S cm^{-1}) in a single crystal.

Results and Discussion

Synthesis. Synthetic methods for **1a** and **1b** were illustrated in Scheme 1. Benzoyl-protected 5-iodouracil derivatives with

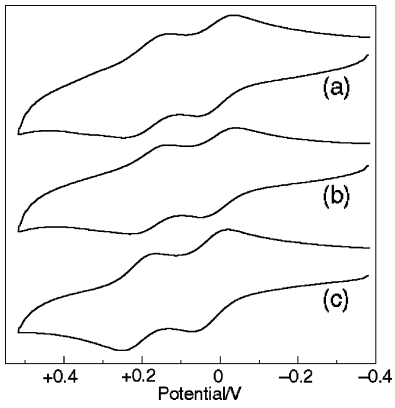

FIGURE 1. Cyclic voltammograms measured in DMF for **1a** (a), **1b** (b), and EDT-TTF (c). For conditions see the Experimental Section.

SCHEME 1. Synthetic Methods for 1a and 1b

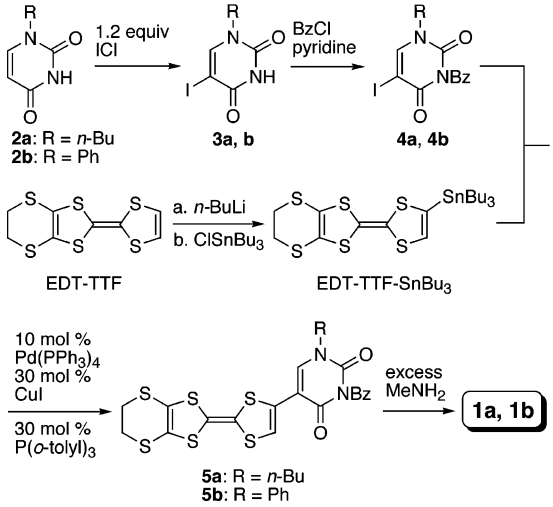

n-butyl and phenyl groups, **4a** and **4b**, were prepared from **2a**[6] and **2b**[10] by iodination and protection of NH groups. Coupling reactions between **4a**, **4b**, and the tributyltin derivative of EDT-TTF (EDT-TTF-SnBu$_3$) produced benzoyl-protected derivatives, **5a** and **5b**. EDT-TTF derivatives, **1a** and **1b**, were synthesized by removal of the benzoyl group of **5a** and **5b** in 29% and 22% yield in three steps form EDT-TTF, respectively. We have found that the benzoyl group facilitates easy purification and enlargement of reaction scale for **5a** and **5b** because of an increase of the solubility for common organic solvents such as CH_2Cl_2 and THF. Furthermore, our present coupling reaction condition in the presence of CuI and P(*o*-tolyl)$_3$ improved the reaction yield compared with that of our previous method for TU and T*n*bU.[11] The CT complexes of **1a** and **1b** with TCNQ were obtained as black powders by mixing both CH_2Cl_2 solutions. Molecular ratios of the TCNQ complexes were found to be 2:1 (D:A) and 2:1:1 (D:A:H_2O), and these complexes are formulated as (**1a**)$_2$−TCNQ and (**1b**)$_2$−TCNQ·H_2O, respectively.

Electron-Donating Ability. The cyclic voltammograms of **1a** and **1b** in DMF exhibit two-stage reversible oxidation waves (Figure 1). Slightly negative shifts of the first oxidation potentials of **1a** and **1b** by 0.01−0.02 V were observed

(4) Morita, Y.; Miyazaki, E.; Fukui, K.; Maki, S.; Nakasuji, K. *Bull. Chem. Soc. Jpn.* **2005**, *78*, 2014.

(5) Murata, T.; Morita, Y.; Fukui, K.; Sato, K.; Shiomi, D.; Takui, T.; Maesato, M.; Yamochi, H.; Saito, G.; Nakasuji, K. *Angew. Chem., Int. Ed.* **2004**, *43*, 6343.

(6) Morita, Y.; Maki, S.; Ohmoto, M.; Kitagawa, H.; Okubo, T.; Mitani, T.; Nakasuji, K. *Org. Lett.* **2002**, *4*, 2185.

(7) As an alternative approach for utilization of nucleobases in the TTF π-system, uracil- and cytosine-fused TTF derivatives are reported. The betaine compounds of these systems exhibited high electrical conductivities as single-component molecular conductors. However, poor solubilities hamper clarification of the crystal structures. See: (a) Neilands, O.; Belyakov, S.; Tilika, V.; Edzina, A. *J. Chem. Soc., Chem. Commun.* **1995**, 325. (b) Neilands, O. Y.; Tilika, V.; Sudmale, I.; Grigorjeva, I.; Edzina, A.; Fonavs, E.; Muzikante, I. *Adv. Mater. Opt. Electron.* **1997**, *7*, 39. (c) Balodis, K.; Khasanov, S.; Chong, C.; Maesato, M.; Yamochi, H.; Saito, G.; Neilands, O. *Synth. Met.* **2003**, *133*−*134*, 353.

(8) Several H-bonded CT salts of EDT-TTF-CONHR (R = H, Me) with metallic behavior were reported. See: (a) Heuzé, K.; Fourmigué, M.; Batail, P.; Canadell, E.; Auban-Senzier, P. *Chem. Eur. J.* **1999**, *5*, 2971. (b) Heuzé, K.; Mézière, C.; Fourmigué, M.; Batail, P.; Coulon, C.; Canadell, E.; Auban-Senzier, P.; Jérome, D. *Chem. Mater.* **2000**, *12*, 1898.

(9) Ono, G.; Terao, H.; Higuchi, S.; Sugawara, T.; Izuoka, A.; Mochida, T. *J. Mater. Chem.* **2000**, *10*, 2277.

(10) Naim, A.; Shevlin, P. B. *Synth. Commun.* **1990**, *60*, 554.

(11) Previous coupling condition for TU and T*n*bU with EDT-TTF-SnBu$_3$ and **4a** and **4b** gave **1a** and **1b** in 20% and 10% yields in three steps, respectively. See ref 6.

TABLE 1. Half-Wave Oxidation Potentials for 1a, 1b, and EDT-TTF[a]

	$E_{1/2}^{ox1}$	$E_{1/2}^{ox2}$	ΔE
1a	+0.00	+0.18	0.18
1b	+0.01	+0.19	0.18
EDT-TTF	+0.02	+0.21	0.19

[a] $Fc/Fc^+ = 0$ V. For conditions, see the Experimental Section.

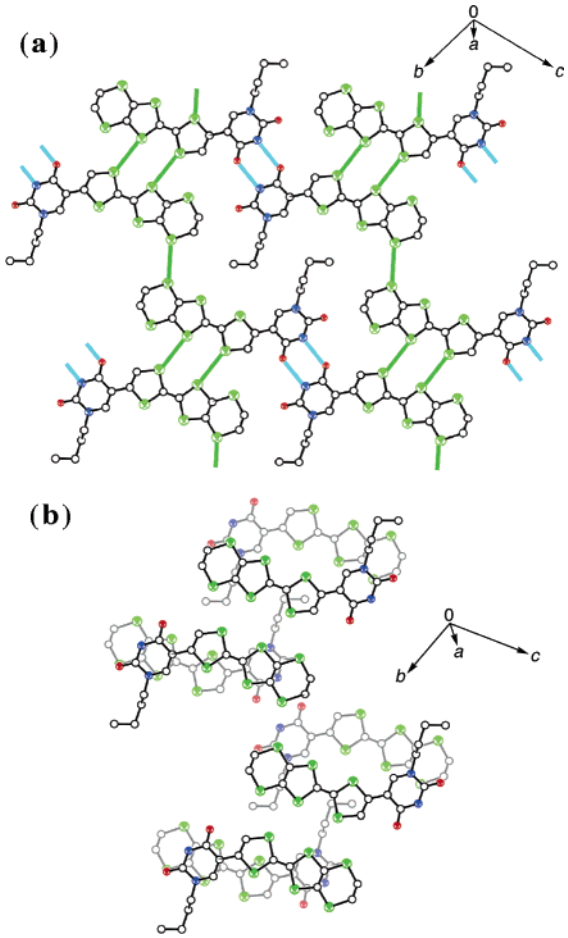

FIGURE 2. Crystal structure of **1a**: two-dimensional sheet structure through Watson−Crick type complementary double H-bonds (blue line) and multiple S···S interactions (greenish yellow line) with the S···S distances of 3.48 and 3.50 Å between TTF moieties and ethylenedithio moieties, respectively (a). The light colored molecular network denotes the sheet of the backward network (b). Hydrogen atoms are omitted for clarity.

compared with that of EDT-TTF, indicating that **1a** and **1b** possess sufficient electron-donating abilities for forming the CT complexes with common organic acceptors (Table 1). Considering approximately the same ΔE values of **1a**, **1b**, and EDT-TTF, the degree of their on-site coulomb repulsion is practically the same.

Crystal Structures of 1a and 1b. Single crystals of **1a** suitable for an X-ray structure analysis were obtained as red blocks by the vapor diffusion method with use of DMF−water, and **1a** crystallizes in a triclinic system, space group $P\bar{1}$. The dihedral angle between the EDT-TTF and uracil moieties is 2.82(7)°. Watson−Crick type complementary double H-bonds through $C^4{=}O{\cdots}H{-}N^3$ in the uracil moieties are formed, in which the closest double NH···O contacts are 2.81 Å (Figure 2a). Furthermore, multiple intermolecular short S···S interactions

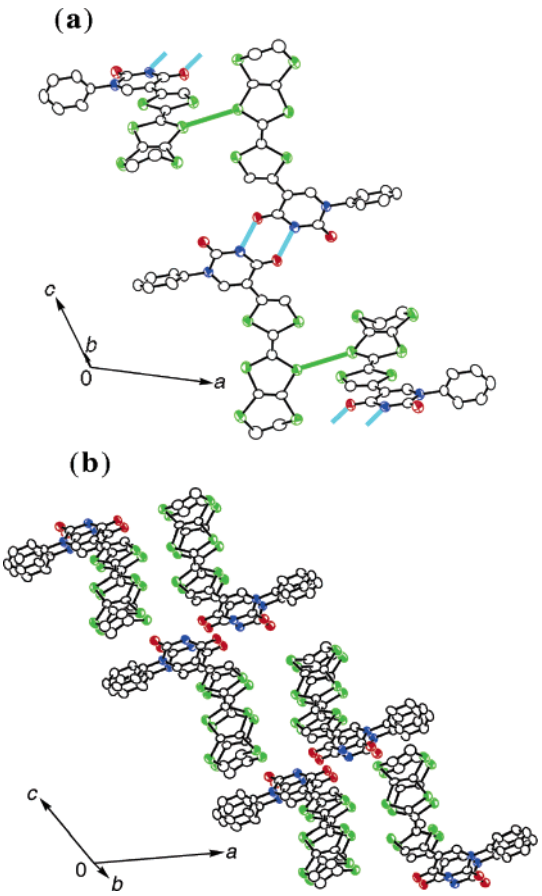

FIGURE 3. Crystal structure of **1b**: chain structure through Watson−Crick type complementary double H-bonds (light blue line) and S···S interaction (greenish yellow line) with the S···S distances of 3.38 Å between the TTF moieties (a) and the two-dimensional layer structure through H-bonding, S···S and $\pi{\cdots}\pi$ interactions with an interplanar distance of 3.38 Å along the *b*-axis (b). Hydrogen atoms are omitted for clarity.

within the sum of van der Waals radii (3.60 Å)[12] are observed between not only the TTF moieties (3.48 Å) but also the ethylenedithio moieties (3.50 Å). Collaboration of these complementary double H-bonds and multiple S···S interactions constructs a two-dimensional sheet structure. Additionally, TTF and uracil moieties are partially overlapped through the $\pi{\cdots}\pi$ interaction with a distance of 3.53 Å (Figure 2b).

Single crystals of **1b** crystallized in a monoclinic system, space group *C*2/*c*, were also obtained by the vapor diffusion method with use of DMF−water. Dihedral angles between EDT-TTF and uracil and those between the uracil moiety and the phenyl group are 11.6(2)° and 115.2(3)°, respectively. In the uracil moiety, an H-bonded dimer connected with Watson−Crick type complementary double H-bonds with an NH···O distance of 2.86 Å is formed (Figure 3a). There is a strong S···S interaction of 3.38 Å between the TTF moieties. Furthermore, the regular stacking structure is formed through the $\pi{\cdots}\pi$ interaction of an interplanar distance of 3.38 Å with partial overlap between TTF and uracil moieties, resulting in formation of a two-dimensional layer structure (Figure 3b).

Crystal Structure of $(\mathbf{1a})_2$−TCNQ. Single crystals of $(\mathbf{1a})_2$−TCNQ were obtained by slow evaporation, using its CH_2Cl_2 solution. The dihedral angle between EDT-TTF and uracil

(12) Bondi, A. *J. Phys. Chem.* **1964**, *68*, 441.

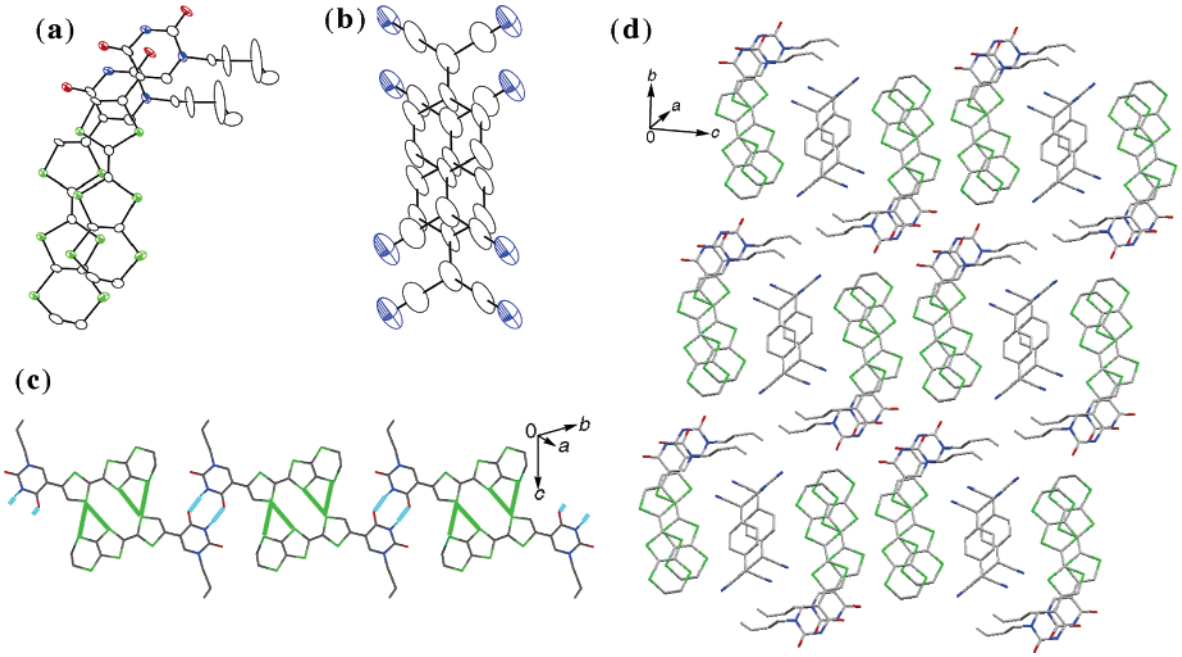

FIGURE 4. Crystal structure of (**1a**)$_2$-TCNQ: overlap modes of **1a** and TCNQ (a, b), one-dimensional chain structure through multiple S···S contacts (greenish yellow line) and Watson−Crick type complementary double H-bonds (blue line) (c), and channel structure constructed by **1a** (d). Hydrogen atoms are omitted for clarity.

moieties is 7.2(2)°. In this TCNQ complex, the segregated stacking structure is formed (Figure 4a,b). Watson−Crick type complementary double H-bonds through C^4═O···H−N^3 in the uracil moieties are formed (NH···O distance: 2.80 Å, see Figure 4c). This H-bonded motif in the uracil moiety is also the same as that of **1a**.[13] These H-bonding natures observed only between electron-donor molecules are rare events as the CT complexes and salts of the TTF derivatives with H-bonded functionality.[14] As expected, there are intermolecular multiple S···S contacts (3.38 and 3.42 Å) between EDT-TTF moieties in the side-by-side direction. In addition to these noncovalent interactions, π···π interaction with an interplanar distance of 3.46 Å is observed between the donor molecules, resulting in construction of the two-dimensional layer structure. The *n*-butyl group of the uracil moiety serves to separate the space between the columns and to construct a channel structure (Figure 4d). The functional channel structure was often shown in the CT salts of TTF derivatives with a metal complex.[15] TCNQ molecules are located in the microporous space of the channel structure. Due to disorder of TCNQ molecules along the stacking direction in the channel, the existence of intermolecular S···N interaction between the donor and the TCNQ molecule is unclear.[16] From the data of the X-ray structure analysis, reflections due to the supercell were not observed in this TCNQ complex.

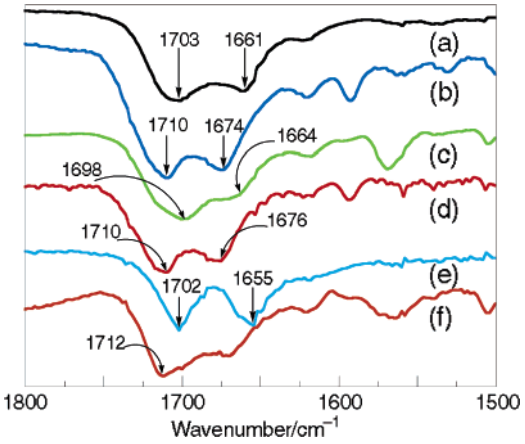

FIGURE 5. Infrared spectra of **1a** (a), **1b** (b), (**1a**)$_2$−TCNQ (c), (**1b**)$_2$−TCNQ·H$_2$O (d), T*n*bU (e), and T*n*bU−TCNQ (f) in KBr pellets.

Optical Properties of TCNQ Complexes of 1a and 1b. The H-bonded motif in the 3,4-positions of the uracil moiety observed by the X-ray crystal structure analyses of **1a**, **1b**, and (**1a**)$_2$−TCNQ is also confirmed by IR spectra in the region of carbonyl stretching frequencies of 1500−1800 cm^{-1} (Figure 5).[17] Two absorption bands at 1661−1674 and 1698−1710 cm^{-1} are assignable to 4- and 2-positions of the uracil moiety, respectively. The carbonyl stretching frequencies of the (**1b**)$_2$−TCNQ·H$_2$O are also observed at 1676 and 1710 cm^{-1}, which

(13) In the TTF-uracil system, transformation of complementary double hydrogen-bonding motifs from Watson−Crick type to revese Watson−Crick type by redox change of the TTF moiety was reported. See: Miyazaki, E.; Morita, Y.; Umemoto, Y.; Fukui, K.; Nakasuji, K. *Chem. Lett.* **2005**, *34*, 1326.

(14) In general, H-bonds tend to form between electron donor and acceptor/counterion/crystal solvent in H-bonded TTF systems. See ref 3.

(15) In {(TTF)$_2$[Fe(CA)$_2$(H$_2$O)$_2$]}$_n$ (H$_2$CA = chloranilic acid), TTF molecules were included in the channel. See: (a) Nagayoshi, K.; Kabir M. K.; Tobita, H.; Honda, K.; Kawahara, M.; Katada, M.; Adachi, K.; Nishikawa, H.; Ikemoto, I.; Kumagai, H.; Hosokoshi, Y.; Inoue, K.; Kitagawa, S.; Kawata, S. *J. Am. Chem. Soc.* **2003**, *125*, 221. Also disordered H_3O^+/NH_4^+ molecules capable of proton conducting were located in the channel formed by the stack of crown ether in (BEDT-TTF)$_4$[(Cat)M^{III}(C$_2$O$_4$)$_3$]$_2$([18]crown-6-ether)]·5H$_2$O (BEDT-TTF = bis(ethylenedithio)-tetrathiafulvalene, Cat = H_3O^+ or NH_4^+). See: (b) Rashid, S.; Turner, S. S.; Day, P.; Light, M. E.; Hursthouse, M. B.; Firth, S.; Clark, R. J. H. *Chem. Commun.* **2001**, 1462. (c) Akutsu-Sato, A.; Akutsu, H.; Turner, S. S.; Day, P.; Probert, M. R.; Howard, J. A. K.; Akutagawa, T.; Takeda, S.; Nakamura, T.; Mori, T. *Angew. Chem., Int. Ed.* **2005**, *44*, 292.

(16) The S···N distance between TCNQ and **1a** obtained by X-ray crystal structure analysis gave 3.03 Å, which is shorter than that of the sum of van der Waals radii (3.35 Å).

(17) We have already discussed the relationship between H-bonded motifs and carbonyl stretching frequencies in the TTF-uracil system. See ref 6.

TABLE 2. Selected Physical Properties for TCNQ Complexes of 1a and 1b

	CN stretching, cm^{-1}	ionicity of TCNQ[a]	CT band, cm^{-1}	σ_{rt}, S cm^{-1}	E_a, meV
(**1a**)$_2$−TCNQ	2193	0.77	4500	2.1[b]	72
(**1b**)$_2$−TCNQ·H_2O	2195	0.73	3000[d]	6.4×10^{-3} [c]	61

[a] Ionicity of the TCNQ molecule was estimated by the CN stretching frequency of the IR spectrum on the basis of Chappell's method. See ref 18. [b] Electric conductivity of a single crystal was measured by a two-probe method. [c] Electric conductivity of a compressed pellet was measured by a four-probe method. [d] See ref 19.

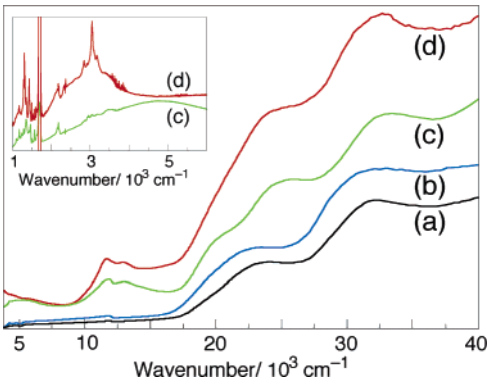

FIGURE 6. Electronic spectra of **1a** (a), **1b** (b), (**1a**)$_2$−TCNQ (c), and (**1b**)$_2$−TCNQ·H_2O (d) in KBr pellets.

are similar values compared with those of **1a**, **1b**, and (**1a**)$_2$−TCNQ. This result indicates that in (**1b**)$_2$−TCNQ·H_2O the formation of Watson−Crick type complementary double H-bonds between the donor molecules is expected as seen in (**1a**)$_2$−TCNQ.

Ionicities of TCNQ molecules were estimated to be 0.77 for (**1a**)$_2$−TCNQ and 0.73 for (**1b**)$_2$−TCNQ·H_2O in terms of the nitrile stretching frequencies of the B_{1u} mode of the IR spectra (Table 2).[18] Considering the molecular ratio of donor and acceptor, the ionicities of **1a** and **1b** in the TCNQ complexes are 0.39 and 0.37, respectively.

In the electronic spectra of (**1a**)$_2$−TCNQ and (**1b**)$_2$−TCNQ·H_2O in KBr pellets, low-energy bands were observed around 4500 and 3000 cm^{-1}, respectively, which is assignable to intrastack CT transition due to the donor and/or acceptor column (Figure 6).[19] The identification of the absorption band around 12 000−14 000 cm^{-1}, however, is less clear. Several possibilities of its origin can be considered: intramolecular transition due to radical anionic species of TCNQ; intermolecular CT transition due to the dimer of the TCNQ molecules; and intermolecular CT transition due to the dimer of the donor molecules.[20,21]

Electric Conductivities of TCNQ Complexes. These TCNQ complexes exhibited semiconductive behaviors with high electric

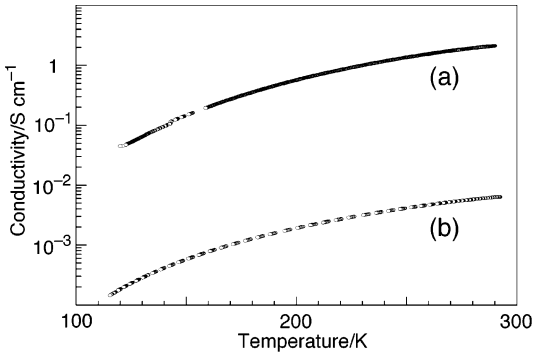

FIGURE 7. Temperature-dependent conductivities for (**1a**)$_2$−TCNQ (a) and (**1a**)$_2$−TCNQ·H2O (b) measured by using a single crystal and a compressed pellet, respectively.

conductivities despite the H-bonded CT complexes.[22] Room temperature electric conductivities (σ_{rt}) and activation energies (E_a) measured by a single crystal and a compressed pellet are determined to be 2.1 S cm^{-1} and 72 meV for (**1a**)$_2$−TCNQ and 6.4×10^{-3} S cm^{-1} and 61 meV for (**1b**)$_2$−TCNQ·H_2O, respectively (Table 2 and Figure 7). Especially, the σ_{rt} value of (**1a**)$_2$−TCNQ is three orders higher than that of the $TCNQF_4$ complex of EDT-TTF-$CONH_2$ with partial CT state.[23] This result of (**1a**)$_2$−TCNQ is in accord with the segregated stacking structure and partial CT states of donor and acceptor molecules (vide supra). Especially, multiple S···S interactions between the EDT-TTF moieties, playing an important role in forming the channel structure, may contribute to high electric conductivity.

Conclusions

The crystal structures of **1a** and **1b** demonstrated that the utilization of *ethylenedithio*-functionalized TTF was an effective way to introduce multiple S···S interactions between donor molecules even in an H-bonded CT system, resulting in construction of a two-dimensional network. Notably, this study has succeeded in solving the first crystal structure of the TCNQ CT complex of the TTF−nucleobase system, (**1a**)$_2$−TCNQ, showing the interplay of complementary double H-bonds, π··· π, and multiple S···S interactions. These features highly contributed to the construction of the layer structure of electron-donor molecules. Furthermore, a key feature of a purely organic system in the structural motif of the (**1a**)$_2$−TCNQ CT complex includes the channel structure containing partially ionized TCNQ columns to show high electric conductivity ($\sigma_{rt} = 2.1$ S cm^{-1}).[24] Interestingly, the uracil moiety serve to form the H-bonded dimer of electron-donor molecules through the Watson−Crick

(18) (a) Chappell, J. S.; Bloch, A. N.; Bryden, W. A.; Maxfield, M.; Poehler, T. O.; Cowan, D. O. *J. Am. Chem. Soc.* **1981**, *103*, 2442. It is noteworthy that an estimation of ionicity of the TCNQ molecule by Chappell's method remains ambiguous, because it often gives inaccurate values in larger ionicity than ~0.5. See: (b) Saito, G.; Hirate, S.; Nishimura, K.; Yamochi, H. *J. Mater. Chem.* **2001**, *11*, 723. (c) Pac, S.-S.; Saito, G. *J. Solid State Chem.* **2002**, *168*, 486.

(19) A CT band of (**1b**)$_2$−TCNQ·H_2O was observed around 3000 cm^{-1} in the IR spectra in KBr pellet. However, this assignment is obscure because of the possibility for overlap of the absorption of water. See IR spectra in the Supporting Information.

(20) Torrance, J. B.; Scott, B. A.; Welber, B.; Kaufman, F. B.; Seiden, P. E. *Phys. Rev.* **1979**, *B19*, 730.

(21) The B bands of the CT process due to the intradimer of the donors in TTF and BEDT-TTF are approximately 14 000 and 10 000 cm^{-1}. Therefore, that of expectable values in EDT-TTF is 12 000 cm^{-1}. See ref 14 and the following: Lapi'nski, A.; Graja, A.; Prokhorova, T. G. *J. Mol. Struct.* **2004**, *704*, 83.

(22) In a variety of H-bonded CT complexes and salts based on the TTF derivatives, most of them exhibited semiconductive behavior with low conductivity below 10^{-5} S cm^{-1} or are insulators except for several examples. See refs 3, 5, 8, and 9.

(23) Partial CT complex of (EDT-TTF-$CONH_2$)$_2$−$TCNQF_4$ with the one-dimensional chain of the electron-donor molecule exhibiting a relatively high conductivity of 3×10^{-3} S cm^{-1} (σ_{rt}) in a single crystal. See: Baudron, S. A.; Mézière, C.; Heuzé, K.; Fourmigué, M.; Batail, P.; Molinié, P.; Auban-Senzier, P. *J. Solid State Chem.* **2002**, *168*, 668.

(24) For a recent review on functional metal coordination polymers with channel structures, see: Kitagawa, S.; Kitaura, R.; Noro, S. *Angew. Chem., Int. Ed.* **2004**, *43*, 2334.

type complementary double N−H···O H-bonds in all EDT-TTF derivatives independent of substituent on uracil and the redox nature of the molecule. Construction of multidimensional networks through noncovalent interactions and achievement of high electric conductivity in the H-bonded CT complex will bring us the beginning of the elucidation and realization of the cooperative proton and electron-transfer process.[25]

Experimental Section[26]

5-Iodo-N^1-phenyluracil (3b). N^1-Phenyluracil[10] (2.5 g, 13 mmol) was placed in a Schlenk tube equipped with a reflux condenser and dissolved with CH_2Cl_2 (15 mL). To this mixture was added iodine chloride (1.4 mL, 27 mmol) and the mixture was refluxed for 1 h. After the solution was cooled at room temperature, the resulting white precipitate was collected by filtration and washed with ether. This residue was recrystallized from ethyl acetate−ethanol (1:1) to give 5-iodo-N^1-phenyluracil (3.3 g, 77%) as a white solid: mp 285−286 °C; TLC R_f 0.64 (ethyl acetate); ^{1}H NMR (270 MHz, DMSO-d_6) δ 7.44 (m, 5H), 8.18 (s, 1H), 11.8 (br s, 1H); IR (KBr) 3165, 3050, 1701, 1675 cm^{-1}; EI-MS, m/z 314 (M^+, 47%). Anal. Calcd for $C_{10}H_7N_2O_2I$: C, 38.24; H, 2.25; N, 8.92. Found: C, 37.97; H, 2.17; N, 8.83.

N^3-Benzoyl-N^1-n-butyl-5-iodouracil (4a). N^1-n-Butyl-5-iodouracil[6] (5.0 g, 17 mmol) was placed in a 100-mL round-bottomed flask and dissolved in CH_3CN (17 mL) and pyridine (7 mL) following addition of benzoyl chloride (4.3 mL, 37 mmol) at room temperature. After the solution was stirred at room temperature for 24 h, the solvents were removed by evaporation, and ethyl acetate (300 mL) and water (100 m) were added. The organic layer was separated and washed with water (100 mL), dried over anhydrous Na_2SO_4, filtered, and concentrated under reduced pressure. The residual yellow oil was recrystallized from hexanes−ethyl acetate to give **4a** (6.5 g, 96%) as a white solid. Mp 129−130 °C; TLC R_f 0.63 (1:1 hexane/ethyl acetate); ^{1}H NMR (270 MHz, DMSO-d_6) δ 0.88 (t, 3, J = 7.3 Hz), 1.21−1.35 (m, 2), 1.55−1.66 (m, 2), 3.73 (t, 2, J = 7.4 Hz), 7.56−7.62 (m, 2), 7.75−7.81 (m, 1), 7.95−7.99 (m, 2), 8.45 (s, 1); IR (KBr) 3074, 1743, 1694, 1662 cm^{-1}; FAB-MS, m/z 399 ($M + H^+$). Anal. Calcd for $C_{15}H_{15}N_2O_3I$: C, 45.24; H, 3.80; N, 7.04. Found: C, 45.24; H, 3.62; N, 7.11.

N^3-Benzoyl-N^1-phenyl-5-iodouracil (4b). 5-Iodo-N^1-phenyluracil (5.1 g, 16 mmol) was placed in a 100-mL round-bottomed flask and dissolved in CH_3CN (20 mL) and pyridine (7 mL) following addition of benzoyl chloride (4.2 mL, 36 mmol) at room temperature. After being stirred at room temperature for 24 h, the solvents were removed by evaporation and ethyl acetate (300 mL) and water (100 m) were added. The organic layer was separated and washed with water (100 mL) and dried over anhydrous Na_2SO_4, filtered, and concentrated under reduced pressure. The residual white solid was recrystallized from hexanes−ethyl acetate, to give **4b** (4.8 g, 69%) as a white solid. Mp 216−218 °C; TLC R_f 0.63 (1:1 hexane/ethyl acetate); ^{1}H NMR (270 MHz, DMSO-d_6) δ 7.35−7.42 (m, 2), 7.44−7.54 (m, 5), 7.63−7.69 (m, 1), 7.91 (s, 1), 7.94−7.99 (m, 2); IR (KBr) 3075, 1743, 1695, 1666 cm^{-1}; FAB-MS, m/z 419 ($M^+ + H$). Anal. Calcd for $C_{17}H_{11}N_2O_3I$: C, 48.83; H, 2.65; N, 6.70. Found: C, 49.09; H, 2.56; N, 6.69.

2-{4-($N^{1'}$-n-Butyluracil-5'-yl)-1,3-dithiole-2-ylidene}-5,6-dihydro-1,3-dithiolo[4,5-b][1,4]dithiin (1a). EDT-TTF[27] (300 mg, 1.0 mmol) was placed in a 100-mL Schlenk tube and dissolved with THF (22 mL). After the solution was cooled at −78 °C, n-BuLi (1.6 M hexane solution, 0.63 mL, 1.0 mmol) was added and the mixture was stirred at −78 °C for 1 h. To this mixture was added tributyltin(IV) chloride (0.29 mL, 1.0 mmol), and the solution was gradually warmed to room temperature. After being stirred for 30 min, a pH 7.0 phosphate buffer solution (0.1 M, 25 mL) was poured, and the reaction mixture was extracted with ethyl acetate (2 × 30 mL). The combined organic extracts were dried over anhydrous Na_2SO_4, then filtered and concentrated under reduced pressure to give the mixture of tributyltin-substituted EDT-TTF (written simply as EDT-TTF-$SnBu_3$) and EDT-TTF (766 mg) as a red oil. This crude oil was used for the next coupling reactions.

The mixture of EDT-TTF-$SnBu_3$ and EDT-TTF (766 mg), **4a** (404 mg, 1.0 mmol), copper(I) iodide (58 mg, 0.30 mmol), and tris(o-tolyl)phosphine (96 mg, 0.30 mmol) were placed in a 50-mL Schlenk tube and dissolved in THF (15 mL). To this mixture was added tetrakis(triphenylphosphine)palladium(0) (117 mg, 0.10 mmol), and the solution was stirred at room temperature for 27 h. After quenching by the addition of water (30 mL), the solution was extracted with ethyl acetate (2 × 40 mL). The combined organic extracts were dried over anhydrous Na_2SO_4, then filtered and concentrated under reduced pressure. The residual powder was purified by silica gel column chromatography with 5:1 hexanes−ethyl acetate and ethyl acetate, to give a mixture of the EDT-TTF derivative with benzoyl-protected butyluracil **5a** and **4a** (516 mg). **5a**: TLC R_f 0.58 (1:1 hexane/ethyl acetate).

The mixture of **5a** and **4a** (516 mg) was placed in a 20-mL Schlenk tube, dispersed in 30% methylamine methanol solution (6 mL), and stirred at room temperature for 30 min. After being cooled at 0 °C, the solution was neutralized by concentrated acetic acid and collected, to give **1a** (137 mg) as a reddish orange powder in 29% yield in three steps from EDT-TTF. Mp 240−241 °C dec; TLC R_f 0.60 (ethyl acetate); ^{1}H NMR (270 MHz, DMSO-d_6) δ 0.90 (t, 3, J = 7.3 Hz), 1.21−1.32 (m, 2), 1.52−1.63 (m, 2), 3.40 (s, 4), 3.73 (t, 2, J = 7.1 Hz), 7.34 (s, 1), 7.87 (s, 1), 11.6 (br s, 1); IR (KBr) 3415, 2954, 1703, 1661 cm^{-1}; UV (KBr) 308, 416 nm; EI-MS m/z 460 (M^+, 71%). Anal. Calcd for $C_{16}H_{16}N_2O_2S_6$: C, 41.71; H, 3.50; N, 6.08. Found: C, 41.59; H, 3.42; N, 5.97.

2-{4-($N^{1'}$-Phenyluracil-5'-yl)-1,3-dithiole-2-ylidene}-5,6-dihydro-1,3-dithiolo[4,5-b][1,4]dithiin (1b). EDT-TTF[27] (100 mg, 0.34 mmol) was placed in a 100-mL Schlenk tube and dissolved in THF (8 mL). After the mixture was cooled at −78 °C, n-BuLi (1.6 M hexane solution, 0.21 mL, 0.34 mmol) was added and the solution was at −78 °C for 1 h. To this mixture was added tributyltin(IV) chloride (0.09 mL, 0.34 mmol), and the solution was gradually warmed to room temperature. After the solution was stirred for 30 min, a pH 7.0 phosphate buffer solution (0.1 M, 15 mL) was added, and the reaction mixture was extracted with ethyl acetate (2 × 30 mL). The combined organic extracts were dried over anhydrous Na_2SO_4, then filtered and concentrated under reduced pressure, to give a mixture of EDT-TTF-$SnBu_3$ and EDT-TTF (255 mg) as a red oil. This crude oil was used for the next coupling reactions.

The mixture of EDT-TTF-$SnBu_3$ and EDT-TTF (255 mg), **4b** (141 mg, 0.34 mmol), copper(I) iodide (19 mg, 0.10 mmol), and tris(o-tolyl)phosphine (32 mg, 0.10 mmol) were placed in a 20-mL Schlenk tube and dissolved with THF (5 mL). To this mixture was added tetrakis(triphenylphosphine)palladium(0) (39 mg, 0.034 mmol), and the solution was stirred at room temperature for 22 h. After quenching by the addition of water (20 mL), the solution was extracted with ethyl acetate (2 × 30 mL). The combined organic extracts were dried over anhydrous Na_2SO_4, then filtered and concentrated under reduced pressure. The residual powder was purified by silica gel column chromatography with 5:1 hexanes−ethyl acetate and ethyl acetate, to give the mixture of EDT-TTF derivative with benzoyl-protected phenyluracil **5b** and **4b** (165 mg). **5b**: TLC R_f 0.63 (1:1 hexane/ethyl acetate).

The mixture of **5b** and **4b** (165 mg) was placed in a 20-mL Schlenk tube, dispersed in 30% methylamine methanol solution (2

(25) Nakasuji, K.; Sugiura, K.; Kitagawa, T.; Toyoda, J.; Okamoto, H.; Okaniwa, K.; Mitani, T.; Yamamoto, H.; Murata, I.; Kawamoto, A.; Tanaka, J. *J. Am. Chem. Soc.* **1991**, *113*, 1862−1864.

(26) See the Experimental Section in the Supporting Information for X-ray crystal structure analyses.

(27) (a) Papavassiliou, G. C.; Mousdis, G. A.; Yiannopoulos, S. Y.; Kakoussis, V. C.; Zambounnis, J. S. *Synth. Met.* **1998**, *27*, B373. (b) Papavassilou, G. C.; Kakoussis, V. C.; Mousdis, G. A.; Gionis, V.; Yiannnopoulos, S. Y. *Mol. Cryst. Liq. Cryst. Incorporating Nonlinear Opt.* **1998**, *156*, 269.

mL), and stirred at room temperature for 30 min. After being cooled at 0 °C, the solution was neutralized by concentrated acetic acid and collected, to give **1b** (36 mg) as a reddish orange powder in 22% yield in three steps from EDT-TTF. Mp 246−248 °C dec; TLC R_f 0.30 (1:1 hexane/ethyl acetate); ^{1}H NMR (270 MHz, DMSO-d_6) δ 3.38 (s, 4), 7.35 (s, 1), 7.41−7.53 (m, 5), 7.82 (s, 1), 11.8 (br s, 1); IR (KBr) 2842, 1710, 1674 cm^{-1}; UV (KBr) 304, 426 nm; EI-MS *m*/*z* 480 (M^+, 18%). Anal. Calcd for $C_{18}H_{12}N_2O_2S_6$: C, 44.97; H, 2.52; N, 5.83. Found: C, 44.88; H, 2.63; N, 5.95.

(1a)$_2$−TCNQ Complex. Both a CH_2Cl_2 solution (30 mL) of **1a** (17.5 mg, 0.038 mmol) and a CH_2Cl_2 solution (10 mL) of TCNQ (7.3 mg, 0.036 mmol) were combined in a 100-mL round-bottomed flask at room temperature, then concentrated under reduced pressure. Residual powder was suspended in a small amount of CH_3CN and collected, to give the (**1a**)$_2$−TCNQ complex (7.1 mg) as a black powder. Mp 215−217 °C dec; IR (KBr) 2212, 2193, 2180, 1698 cm^{-1}; UV (KBr) 300, 386, 768, 838 nm. Anal. Calcd for $(C_{16}H_{16}N_2O_2S_6)_2(C_{12}H_4N_4)$: C, 46.95; H, 3.22; N, 9.95. Found. C, 46.65; H, 3.14; N, 9.83.

(1b)$_2$−TCNQ·H$_2$O Complex. Both a CH_2Cl_2 solution (130 mL) of **1b** (57 mg, 0.12 mmol) and a CH_2Cl_2 solution (20 mL) of TCNQ (12 mg, 0.056 mmol) were combined in a 300-mL round-bottomed flask at room temperature, then concentrated under reduced pressure. Precipitates were collected, to give the (**1b**)$_2$−TCNQ·H_2O complex (27 mg) as a black powder. Mp 269−271 °C dec; IR (KBr) 2214, 2195, 2178, 2154, 1710, 1676 cm^{-1}; UV (KBr) 306, 774, 856 nm. Anal. Calcd for $(C_{18}H_{12}N_2O_2S_6)_2(C_{12}H_4N_4)(H_2O)$: C, 48.71; H, 2.55; N, 9.47. Found: C, 48.83; H, 2.61; N, 9.14. The composition of this TCNQ complex was solely determined by the elemental analysis.

Acknowledgment. This work was partially supported by PRESTO-JST, Grant-in-Aid for Scientific Research (No. 16350074) from the Ministry of Education, Culture, Sports, Science, and Technology, Japan, 21COE program "Creation of Integrated EcoChemistry of Osaka University", and by a grant of the Asahi Glass Foundation.

Supporting Information Available: General experimental information for X-ray crystal structure analyses, list of X-ray crystallographic data for **1a**, **1b**, and (**1a**)$_2$−TCNQ complex in CIF format, and Ortep diagram and IR spectra. This material is available free of charge via the Internet at http://pubs.acs.org.

JO060748L